# Zika virus subversion of chaperone GRP78/BiP expression in A549 cells during UPR activation

Jonathan Turpin, Étienne Frumence, Wissal Harrabi, Juliano Haddad, Chaker El Kalamouni, Philippe Desprès, Pascale Krejbich-Trotot, Wildriss Viranaicken

Research Paper

# Zika Virus subversion of chaperone GRP78/BiP expression in A549 cells during UPR activation

Jonathan Turpin †, Etienne Frumence †, Wissal Harrabi, Juliano G Haddad, Chaker El Kalamouni, Philippe Desprès, Pascale Krejbich-Trotot * and Wildriss Viranaïcken *

Université de La Réunion, INSERM UMR 1187, CNRS 9192, IRD 249, PIMIT, Processus Infectieux en Milieu Insulaire Tropical, Plateforme CYROI, 2, rue Maxime Rivière, 97490 Sainte-Clotilde, Ile de La Réunion. France.

*Correspondence: wildriss.viranaicken@univ-reunion.fr (W.V.); pascale.krejbich@univ-reunion.fr (P.K.T.); Tel.: +33-262938829

† Contribute equally to this work.

**Abstract:** Flaviviruses replicate in membranous factories associated with the endoplasmic reticulum (ER). Significant levels of flavivirus polyprotein integration contribute to ER stress and the host cell may exhibit an Unfolded Protein Response (UPR) to this protein accumulation, stimulating appropriate cellular responses such as adaptation, autophagy or cell death. These different stress responses support other antiviral strategies initiated by infected cells and can help to overcome viral infection. In epithelial A549 cells, a model currently used to study the flavivirus infection cycle and the host cell responses, all three pathways leading to UPR are activated during infection by Dengue virus (DENV), Yellow Fever virus (YFV) or West Nile virus (WNV). In the present study, we investigated the capacity of ZIKA virus (ZIKV) to induce ER stress in A549 cells. We observed that the cells respond to ZIKV infection by implementing an UPR through activation of the IRE1 and PERK pathway without activation of the ATF6 branch. By modulating the ER stress response, we found that UPR inducers significantly inhibit ZIKV replication. Interestingly, our findings provide evidence that ZIKV could manipulate the UPR to escape this host cell defence system by downregulating GRP78/BiP expression. This subversion of GRP78 expression could lead to unresolved and persistent ER stress which can be a benefit for virus growth.

**Keywords:** Zika virus ; Unfolded Protein Response ; Persistent ER stress ; viral growth.

## 1. Introduction

ZIKA virus (ZIKV) is a pathogenic single-stranded RNA virus belonging to the *Flaviviridae* family together with DENV, WNV and JEV. Among the pathogenic flaviviruses, ZIKV has gained notoriety in the last ten years, due to explosive outbreaks and serious clinical concerns. Neurological complications have been described, including Guillain-Barré syndrome (GBS) and congenital malformations, prompting specific vigilance for pregnant women in the event of a Zika epidemic [1,2]. Due to these atypical clinical manifestations, the ability of ZIKV to be transmitted sexually in addition to being vector-borne, and the evidence of its persistence in some tissues, increasing numbers of molecular and cellular studies had

focused on specific ZIKV-host interactions that distinguish it from other flaviviruses. Similar to other flaviviruses, ZIKV replication occurs in Endoplasmic Reticulum (ER) invaginations of infected cells and leads to an accumulation of viral proteins [3–5]. Genome translation is followed by proteolytic cleavage of a polyprotein incorporated into the ER into three structural (C, M, and E) and seven non-structural (NS1, NS2A, NS2B, NS3, NS4A, NS4B, and NS) viral proteins. The ER is thus an essential cellular compartment for the completion of the viral cycle, in addition to several key mechanisms in cell physiology. The standard function of the ER is to regulate folding and post-translational modification of proteins that are to be transported within the cell, or secreted. The correct folding of proteins depends on the N-linked protein glycosylation, the oxidative environment in the ER lumen which promotes the formation of disulfide bonds, and the presence of several $Ca^{2+}$-dependent molecular chaperones (calreticulin, GRP78 also named BiP and GRP94) which stabilize protein folding intermediates [6,7]. ER homeostasis can be perturbed in the case of glucose starvation, hypoxia, calcium dysregulation or following a protein accumulation which will in turn provoke ER stress. The Unfolded Protein Response (UPR) is activated in response to ER stress, in an attempt to restore ER homeostasis. In cells infected by a virus, the huge and sudden accumulation of viral proteins that are processed in the ER usually results in ER stress and the induction of the UPR. This cell response has been shown to be involved in several modes of cell defence, i.e. antiviral programs, immune responses [8,9] and commitment in autophagy or cell suicide [10,11]. During ER stress, the folding chaperone GRP78/BiP dissociates from three ER-resident transmembrane proteins i.e. PKR-like endoplasmic reticulum kinase (PERK), Inositol-Requiring Enzyme 1 (IRE1) and activating transcription factor 6 (ATF6) [12]. Each of these proteins acts as a stress transducer in independent pathways devoted to stress resolution. The activated kinase activity of PERK results in phosphorylation of eIF2α, followed by a transitory translational attenuation and consequently reduced ER influx of newly synthesized proteins. The endonuclease activity of activated IRE1 produces a spliced form of the x-box binding protein 1 (xbp1) transcript. This spliced xbp1 encodes a transcription factor that promotes the expression of genes coding for several factors aimed at resolving ER stress. ATF6 can egress from the ER to the Golgi apparatus for maturation by S1P or S2P cleavage to generate ATF6f. ATF6f acts in the nucleus where it regulates UPR target gene expression. The transcriptional activity of ATF6 and Xbp1 leads to increased expression of chaperones and proteins implicated in enhanced folding capacity or in ER-associated protein degradation (ERAD). In spite of the implementation of an UPR with these adaptive mechanisms, an excessive, unresolved or prolonged ER stress will result in cellular autophagy or apoptosis [13]. Crosstalk between ER stress, UPR, autophagy and apoptosis pathways are of particular importance in the case of virally infected cells since each of these responses will influence the infected cell's health and contribute to determining the efficacy of viral replication and spread.

It has previously been shown that ZIKV has the ability to initiate a UPR response to ER stress in several cell types (Table S1) [14–18] and that infection is accompanied by morphological modification of cellular organelles [19]. However, it is important to decipher how ER stress initiation is mediated, which branches of the UPR pathways are involved and how pathway crosstalk is mediated during cellular and ER responses to ZIKV infection. In epithelial A549 cells, a widely *in vitro* used cell line to characterize cell responses to flavivirus infection (DENV, WNV, JEV), all three branches of the UPR are activated (PERK, ATF6 and IRE1) and associated with enhanced GRP78/BiP expression [20–23]. In this present work, we followed ER stress and the UPR in A549 cells in order to identify mechanisms that could be specific to

ZIKV infection and that may lead to new "*in cellulo*" approaches for understanding clinical outcomes. Imaging of infected A549 cells shows a morphological change typical of ER stress. When we looked at the stress transduction mechanisms, we discovered that the UPR was initiated by the host cell but with no induction of GRP78 expression. This was unexpected regarding previous observations with other flaviviruses including DENV, JEV and WNV [21,23,24]. Considering that UPR pre-activation can limit ZIKV infectious capacity [9], we hypothesized that a partial or impaired UPR could be beneficial for the virus and showed that exogenously-induced UPR was also detrimental to ZIKV at the post entry step. ZIKV would thus have the ability to modulate UPR to its benefits with a mechanism that remains to be discovered.

## 2. Materials and Methods

### 2.1. Virus, Cell culture, antibodies and reagents

The clinical isolate PF-25013-18 (PF13) of ZIKV [25] was used for all infections. A549 cells (ATCC, CCL-185) were cultured at 37 °C under a 5% CO2 atmosphere in MEM medium supplemented with 10% heat-inactivated foetal bovine serum (FBS). Plaque assays were used for viral progeny quantification as described previously [26]. Cellular damages were evaluated measuring a released lactate dehydrogenase (LDH) activity in cell culture supernatants resulting from a plasma membrane rupture. Supernatants of infected cells were collected and subjected to a cytotoxicity assay, performed using CytoTox 96® non-radioactive cytotoxicity assay (Promega) according to manufacturer's instructions. Absorbance of converted dye was measured at 490 nm using a microplate reader (Tecan).

Immunodetection of the viral proteins was performed using the mouse anti-pan flavivirus envelope E protein mAb 4G2, produced by RD Biotech, or with the rat anti-EDIII ZIKV which was described previously [27]. The rabbit anti-Calnexin antibody was purchased from Santa-Cruz Biotechnology (Clinisiences, Nanterre, France). Donkey anti-mouse Alexa Fluor 488 and anti-rabbit Alexa Fluor 594 IgG antibodies were from Invitrogen (Thermofisher, Les Ulis, France). Horseradish peroxidase-conjugated anti-rabbit (ab97051) and anti-mouse (ab6789) antibodies were from Abcam (Cambridge, UK). The antibody against GRP78/Bip (#3177) was from cell Signalling Technology (Ozyme, Saint-Cyr-l'École, France. Thapsigargin (TG), an endoplasmic reticulum $Ca^{2+}$-ATPase inhibitor and Tunicamycin (TM) an inhibitor of N-glycosylation were used to induce ER stress and UPR respectively at 1 µM and 2 $\mu g.mL^{-1}$ for the indicated time in figure legends. These inhibitors were from Sigma-aldrich (Humeau, La Chapelle-Sur-Erdre, France).

### 2.2. Luciferase Reporter assay

Plasmids with GRP94 and GRP78 promoters upstream of F-Luc (pGRP78-Luc and pGRP94-Luc) were provided by Dr. Kazutoshi Mori [28]. One million cells were transfected with the indicated plasmids using Lipofectamine 3000 according to manufacturer instructions (Invitrogen, Thermofisher, Les Ulis, France), incubated for 12 h and then divided into three separate flasks. The first flask was mock treated, the second was infected with ZIKV PF13 at an MOI of 5 for 24h and the third was treated with thapsigargin (1µm) for 6 hours. Luciferase activities were measured using the Luciferase Glo™ assay according to manufacturer's instructions (Promega, Madison, USA).

2.3. Western blot

Cells were grown on 6 well plates at $3.10^6$ cells/well and infected and/or treated with UPR inducer for the indicated time. Then, the cells were washed with PBS and lysed with 300 µL of Radioimmunoprecipitation assay buffer RIPA buffer (Sigma-aldrich Humeau, La Chapelle-Sur-Erdre, France). Total cell extracts were proceeded for western blot as before [27].

2.4. Immunofluorescence

A549 cells were grown, infected or treated on glass coverslips. They were further fixed with 3.7% formaldehyde at room temperature for 10 min. Fixed cells were permeabilized with 0.1% Triton X-100 in PBS for 5 min. Coverslips were incubated with primary antibodies (1:1000 dilution) in 1x PBS 1% BSA for two hours and with Alexa Fluor-conjugated secondary antibodies (1:1000, Invitrogen) for one hour. Nucleus morphology was revealed by DAPI staining. The coverslips were mounted with VECTASHIELD® (Clinisciences, Nanterre, France) and fluorescence was observed using a Nikon Eclipse E2000-U microscope. Images were captured and processed using a Hamamatsu ORCA2 ER camera and the imaging software NIS-Element AR (Nikon, Tokyo, Japan).

2.5. RT-PCR

Semi quantitative RT-PCR and real time qPCR experiments were performed as before [22]. Primers used for RT-PCR were CHOP: F 5'-GCACCTCCCAGAGCCCTCACTCTCC-3′, R 5′-GTCTACTCCAAGCCTTCCCCCTGCG-3′; GRP78: F 5′-CATCACGCCGTCCTATGTCG-3′, R 5′-CGTCAAAGACCGTGTTCTCG-3′; XBP1: F 5'-CCTTGTAGTTGAGAACCAGG-3', R 5'-GGGGCTTGGTATATATGTGG-3'; NS1: F 5′-AGAGGACCATCTCTGAGATC-3', R 5′-GGCCTTATCTCCATTCCATACC-3'; GAPDH: F 5′-GGGAGCCAAAAGGGTCATCA-3', R 5′-TGATGGCATGGACTGTGGTC-3'. ZIKV-E: F 5'-GTCTTGGAACATGGAGG-3', R 5'-TTCACCTTGTGTTGGGC-3'

For semi quantitative RT-PCR, PCR products were analyzed on a 1.5% agarose gel electrophoresis and stained as described before [25].

For Real time, Total RNA including genomic viral RNA was extracted from cells with RNeasy kit (Qiagen) and reverse transcribed using E reverse primer and M-MLV reverse transcriptase (Life Technologies, Villebon-sur-Yvette, France) at 42 °C for 50 min. Quantitative PCR was performed on a CFX96 Real-Time PCR Detection System (Bio-Rad). Briefly, cDNA was amplified using 0.2 µM of each primer and GoTaq Master Mix (Promega, Charbonnières-les-bains, France). For each single-well amplification reaction, a threshold cycle (Ct) was calculated using the CFX96 program (Bio-Rad, Life Science, Marnes-la-Coquette, France) in the exponential phase of amplification. A synthetic gene coding for nucleotides 954 to 1306 of the MR766 strain (GenBank: LC002520) cloned in the pUC57 plasmid was used as template to generate a standard curve, which then served to make absolute quantitation of viral RNA copies in infected cells.

2.6. Statistical analysis

All values are expressed as mean ± SD of at least three independent experiments, as indicated in the figure legends. After normality tests, comparisons between different

treatments were analyzed using a one-way ANOVA. Values of $p<0.05$ were considered statistically significant for a post-hoc Tukey's test. All statistical tests were done using the software Graph-Pad Prism version 7.01.

## 3. Results and discussion

A549 epithelial cells have been shown to be permissive to infection by most flaviviruses [25,30] and are a suitable model for studying *in cellulo* host-virus interactions. Many research teams, including ours, have used this epithelial cell line to characterize ZIKV infection with different strains of the epidemic (clinical isolate PF13, molecular clone BR15) and historical (MR766) ZIKV, deciphering viral entry pathways, viral replication kinetics [31] and cellular responses such as apoptosis [32]. As protein load increases in cells replicating the virus, resulting in the accumulation of misfolded or partially processed viral polyproteins and ER stress, we investigated markers of ER stress and the contribution of the Unfolded Protein Response during the course of ZIKV infection.

### 3.1. ZIKV infection induces ER morphological changes.

When stressed, the ER exhibits morphological abnormalities with luminal swelling and membrane expansion [33]. These morphological changes can be observed by fluorescence microscopy. When we compared Calnexin expression, a standard ER marker, between A549 cells infected for 48 hours with the epidemic strain of ZIKV (PF13) and control (mock infected cells), we noticed morphological shape changes of the ER with obvious swelling and increased calnexin staining (Figure 1). Imaging of the infected cells also showed the colocalization of immunodetected viral envelope protein (E-ZIKV) and calnexin, confirming that viral proteins are present in the enlarged and globe-shaped compartment of an expanding ER (Figure 1).

### 3.2. Unfolded Protein Response during ZIKV infection in A549 cells

Upon ER stress, cells initiate an UPR to prevent persistent damage due to stress and to restore ER homeostasis. In order to decipher the stress transduction mechanisms induced upon ZIKV infection in A549 cells, we analyzed each of the three main UPR pathways. For this purpose, we investigated the expression level of target genes specific to each activated branch.

#### 3.2.1. Effect of ZIKV infection on PERK and IRE1 pathways of UPR.

Activation of the PERK pathway results in eIF2α phosphorylation which is followed by a reduced translation rate. It also leads to ATF4 upregulation. ATF4 is a transcription factor acting on several targets among which is the C/EBP homologous protein (CHOP) encoding gene. CHOP factor plays a key role in stress resolution and in relationships between UPR, cell survival or cell death. We therefore followed activation of this PERK/ATF4 branch by a measure of the expression level of the CHOP gene by RT-PCR (Figure 2A). Effective upregulation of CHOP at the transcriptional level suggests that the PERK branch of UPR was activated during ZIKV infection of A549 cells. This observation is in agreement with previous findings in ZIKV infected human neural stem cells [14].

The IRE1 pathway is characterized by the splicing of the Xbp1-transcript. The spliced Xbp1 (s-Xbp1) encodes a transcription factor able to transactivate genes mainly involved in ERAD. Splicing of Xbp1 was then followed by RT-PCR as an indicator of IRE1 branch activation. s-Xbp1 was detected upon ZIKV infection like in cells treated with thapsigargin (TG), an endoplasmic reticulum $Ca^{2+}$-ATPase inhibitor that is an ER stress and UPR inducer (Figure 2A). The observation of IRE branch activation by ZIKV was also in accordance with previous findings [10].

3.2.2. Effect of ZIKV infection on ATF6 branch of UPR

The third branch of the UPR is mediated by the maturation of ATF6 upon S1P or S2P processing in the Golgi apparatus. Once translocated to the nucleus, mature ATF6 upregulates the expression of chaperone encoding genes like GRP78 (Bip) and GRP94. Increased levels of these chaperones, involved in the refolding of proteins, plays a crucial role in the resolution of ER stress. Unlike thapsigargin treatment of A549 cells, RT-PCR results revealed that grp78 was not upregulated at the transcriptional level during ZIKV infection (Figure 2A). This observation is potentially important as it could be one of the specific interactions of ZIKV that differentiates it from other flaviviruses. Indeed, until now, studies of the UPR response to flavivirus infections, such as for DENV, report the ability of the infected cells to induce grp78 transcription in this A549 model [22].

We further investigated this lack of GRP78 upregulation by two approaches. We first checked the GRP78 protein levels by western blot in cells that were infected for 48h at increasing ZIKV MOI (1, 5 and 10). No modulation of GRP78 expression could be detected under any of these conditions (Figure 2B).

In a second approach, we monitored chaperone induction using luciferase reporter constructs during ZIKV infection. We transfected A549 cells with plasmids encoding a F-Luc reporter gene downstream of grp78 or grp94 promoter. These two promoters contain the ER stress response element (ERSE) which is transactivated by ATF6. Thapsigargin induced expression of the F-Luc reporter gene under control of ERSE for both grp78 and grp94 constructs. This was not the case after ZIKV infection (Figure 2C).

Together these results suggest that ZIKV infection provides a partial transduction of the ER stress with activation of the PERK/ATF4 and IRE1 pathways of the UPR but without any involvement of ATF6. Incomplete or delayed re-folding chaperone induction due to this missing branch of UPR could impact the adaptive response and lead to persistent ER stress. This could also interplay with programmed cell death by signaling pathways downstream of PERK activation with CHOP-mediated regulation of proteins involved in apoptosis like BIM, Bcl-2 and PUMA [34].

3.3. ZIKV controls the UPR pathway to promote viral growth

3.3.1. Activation of the UPR-dependent signaling pathway influences viral growth

ER stress can be induced by the action of tunicamicyn (TM), an inhibitor of N-glycosylation. The resulting UPR can be qualified as ‘standard’ with activation of the PERK, IRE1 and ATF6 pathways [35]. To assess the effect of exogenous activation of UPR on ZIKV infection, we

added this inducer to infected cells 2h after ZIKV inoculation. Cells were harvested and cell culture supernatant collected after 16h of treatment with TM.

We showed that TM treatment during the ZIKV infection of A549 cells was able to significantly inhibit the virus replication. Reduced amounts of viral RNA were related to tunicamycin concentration (Figure 3A). We then confirmed that UPR induction with Tunicamycin impaired viral progeny production by at least 1 log as compared to mock-treated cells (Figure 3B). As expected, the TM-mediated inhibition of viral growth was associated to a lower expression level of ZIKV E protein in a TM dose-dependent manner (Figure 3C). To exclude the possibility that antiviral effect of TM was related to cell death upon infection or treatment, the amount of released LDH was measured in cell culture supernatants (Figure 3B). Using thapsigargin (TG), a UPR inducer that works by alteration of $Ca^{2+}$ homeostasis, or dithiothreitol (DTT), a UPR inducer that works by blocking disulfide bond formation, incubated with infected cells for 16h, 2h after ZIKV inoculation, we observed the same inhibition of ZIKV infection (Figure S1). These observations suggest that a 'standard' UPR has the ability to interfere with ZIKV replication efficiency, independently of the nature of the UPR inducer and even after the post-entry step. This result complements previous findings that pre-activating the UPR response decreases flavivirus titers [9]. However, in the mentioned study, the antiviral effect of the UPR relied on an early activation, by priming an IFN regulatory factor 3-dependent innate immune signaling. In our case, since the UPR inducer is added 2 hours after virus addition, the mechanism that limits infection should be different and exerted on a virus cycle already in progress.

3.3.2. The UPR-dependent activation of GRP78/BiP is counterbalanced by ZIKV

Given that ZIKV infection of A549 cells causes ER-stress leading to UPR activation without ATF6 branch activation nor GRP78/BiP chaperone expression, we asked whether ZIKV counteracts the UPR pathway to promote viral replication. To investigate this issue, ZIKV-infected cells were incubated with TG for 4h and cell lysates were examined for GRP78 expression by Western blot (Figure 3D). As it has been observed with TM, a short treatment with TG resulted in a dramatic reduction in the expression level of ZIKV E protein. This confirms that ZIKV replication is affected by UPR activation in A549 cells. We noted that GRP78 expression was undetectable in A549 cells infected with ZIKV as above (Figure 3D). In contrast to what it has been observed when A549 cells were incubated with TG, TG treatment resulted in a minor change on GRP78 protein expression in cells in which ZIKV replication has been initiated (Figure 3D). Taken together these results would suggest that ZIKV has developed a capacity to control the UPR pathway to its own benefit with a downregulation of GRP78/BiP expression.

5. Conclusions

Our study showed that ZIKV infection of epithelial A549 cells could trigger ER stress. We confirmed the activation of the UPR in this cell model but found that, unlike other flaviviruses [37], ZIKV does not activate all three branches of the UPR stress response. In addition, we found that the UPR can affect ZIKV cellular replication efficiency, but that ZIKV can interfere with the UPR achievement by modulating GRP78 expression. Therefore, we hypothesize that persistent ER stress is induced by ZIKV infection and exploited by the virus to increase its replication that would otherwise be controlled by UPR induction.

**Author Contributions:** conceptualization, W.V., P.K.-T. ; methodology, J.T., E.F., W.V., P.K.-T.; validation, J.T., E.F., W.V., P.K.-T. ; formal analysis, J.T., E.F, W.H., J-G.H., C.E.K., P.D., W.V., P.K.-T. ; investigation, J.T., E.F., W.H., J-G.H., C.E.K.,W.V., P.K.-T. ; resources, P.D., W.V., P.K.-T.; data curation, J.T., E.F, P.D., W.V., P.K.-T.; writing—original draft preparation, J.T., E.F, P.D., W.V., P.K.-T.; writing—review and editing, J.T., E.F, P.D., W.V., P.K.-T.; visualization, W.V., P.K.-T.; supervision, W.V., P.K.-T.; project administration, P.D., W.V., P.K.-T.; funding acquisition, P.D.

**Funding:** This work was supported by the ZIKAlert project (European Union-Région Réunion program under grant agreement n° SYNERGY: RE0001902). E.F. holds a fellowship from the Regional Council of Reunion Island (European Union-Région Réunion program under grant agreement n° SYNERGY: RE0012406). J.T. has a PhD degree scholarship from La Réunion Island University (Ecole Doctorale STS), funded by the French ministry MEESR. J-G.H. received funding from the ZIKAlert program.

**Acknowledgments:** We thank the members of PIMIT and DéTROI laboratories for helpful discussions. We are grateful to Dr. Steeve Bourane and Dr. David A. Wilkinson for the critical review and improvements made to the use of the English language throughout the text. Also, Dr. Kazutoshi Mori, from Kyoto University, for providing us pGRP78-Luc and pGRP94-Luc plasmids.

**Conflicts of Interest:** The authors declare no conflict of interest.

References

[1] Z. Wen, H. Song, G. Ming, How does Zika virus cause microcephaly?, Genes Dev. 31 (2017) 849–861. https://doi.org/10.1101/gad.298216.117.

[2] J. Miranda, D. Martín-Tapia, Y. Valdespino-Vázquez, L. Alarcón, A. Espejel-Nuñez, M. Guzmán-Huerta, J.E. Muñoz-Medina, M. Shibayama, B. Chávez-Munguía, G. Estrada-Gutiérrez, S. Lievano, J.E. Ludert, L. González-Mariscal, Syncytiotrophoblast of Placentae from Women with Zika Virus Infection Has Altered Tight Junction Protein Expression and Increased Paracellular Permeability, Cells. 8 (2019) 1174. https://doi.org/10.3390/cells8101174.

[3] M. Cortese, S. Goellner, E.G. Acosta, C.J. Neufeldt, O. Oleksiuk, M. Lampe, U. Haselmann, C. Funaya, N. Schieber, P. Ronchi, M. Schorb, P. Pruunsild, Y. Schwab, L. Chatel-Chaix, A. Ruggieri, R. Bartenschlager, Ultrastructural Characterization of Zika Virus Replication Factories, Cell Rep. 18 (2017) 2113–2123. https://doi.org/10.1016/j.celrep.2017.02.014.

[4] L. Miorin, I. Romero-Brey, P. Maiuri, S. Hoppe, J. Krijnse-Locker, R. Bartenschlager, A. Marcello, Three-dimensional architecture of tick-borne encephalitis virus replication sites and trafficking of the replicated RNA, J. Virol. 87 (2013) 6469–6481. https://doi.org/10.1128/JVI.03456-12.

[5] I. Romero-Brey, R. Bartenschlager, Membranous Replication Factories Induced by Plus-Strand RNA Viruses, Viruses. 6 (2014) 2826–2857. https://doi.org/10.3390/v6072826.

[6] Z. Sun, J.L. Brodsky, Protein quality control in the secretory pathway, J. Cell Biol. (2019) jcb.201906047. https://doi.org/10.1083/jcb.201906047.

[7] L.M. Hendershot, The ER function BiP is a master regulator of ER function, Mt. Sinai J. Med. N. Y. 71 (2004) 289–297.

[8] J.A. Smith, A new paradigm: innate immune sensing of viruses via the unfolded protein response, Front. Microbiol. 5 (2014). https://doi.org/10.3389/fmicb.2014.00222.

[9] T. Carletti, M.K. Zakaria, V. Faoro, L. Reale, Y. Kazungu, D. Licastro, A. Marcello, Viral priming of cell intrinsic innate antiviral signaling by the unfolded protein response, Nat. Commun. 10 (2019) 3889. https://doi.org/10.1038/s41467-019-11663-2.

[10] A.-B. Blázquez, E. Escribano-Romero, T. Merino-Ramos, J.-C. Saiz, M.A. Martín-Acebes, Stress responses in flavivirus-infected cells: activation of unfolded protein response and autophagy, Front. Microbiol. 5 (2014). https://doi.org/10.3389/fmicb.2014.00266.

[11] R. Sano, J.C. Reed, ER stress-induced cell death mechanisms, Biochim. Biophys. Acta. 1833 (2013) 3460–3470. https://doi.org/10.1016/j.bbamcr.2013.06.028.

[12] B.M. Gardner, D. Pincus, K. Gotthardt, C.M. Gallagher, P. Walter, Endoplasmic reticulum stress sensing in the unfolded protein response, Cold Spring Harb. Perspect. Biol. 5 (2013) a013169. https://doi.org/10.1101/cshperspect.a013169.

[13] A. Almanza, A. Carlesso, C. Chintha, S. Creedican, D. Doultsinos, B. Leuzzi, A. Luís, N. McCarthy, L. Montibeller, S. More, A. Papaioannou, F. Püschel, M.L. Sassano, J. Skoko, P. Agostinis, J. de Belleroche, L.A. Eriksson, S. Fulda, A.M. Gorman, S. Healy, A. Kozlov, C. Muñoz-Pinedo, M. Rehm, E. Chevet, A. Samali, Endoplasmic reticulum stress signalling - from basic mechanisms to clinical applications, FEBS J. 286 (2019) 241–278. https://doi.org/10.1111/febs.14608.

[14] I. Gladwyn-Ng, L. Cordón-Barris, C. Alfano, C. Creppe, T. Couderc, G. Morelli, N. Thelen, M. America, B. Bessières, F. Encha-Razavi, M. Bonnière, I.K. Suzuki, M. Flamand, P. Vanderhaeghen, M. Thiry, M. Lecuit, L. Nguyen, Stress-induced unfolded protein response contributes to Zika virus-associated microcephaly, Nat. Neurosci. 21 (2018) 63–71. https://doi.org/10.1038/s41593-017-0038-4.

[15] C. Alfano, I. Gladwyn-Ng, T. Couderc, M. Lecuit, L. Nguyen, The Unfolded Protein Response: A Key Player in Zika Virus-Associated Congenital Microcephaly, Front. Cell. Neurosci. 13 (2019) 94. https://doi.org/10.3389/fncel.2019.00094.

[16] S. Hou, A. Kumar, Z. Xu, A.M. Airo, I. Stryapunina, C.P. Wong, W. Branton, E. Tchesnokov, M. Götte, C. Power, T.C. Hobman, Zika Virus Hijacks Stress Granule Proteins and Modulates the Host Stress Response, J. Virol. 91 (2017). https://doi.org/10.1128/JVI.00474-17.

[17] R. Amorim, A. Temzi, B.D. Griffin, A.J. Mouland, Zika virus inhibits eIF2α-dependent stress granule assembly, PLoS Negl. Trop. Dis. 11 (2017) e0005775. https://doi.org/10.1371/journal.pntd.0005775.

[18] G. Bonenfant, N. Williams, R. Netzband, M.C. Schwarz, M.J. Evans, C.T. Pager, Zika Virus Subverts Stress Granules To Promote and Restrict Viral Gene Expression, J. Virol. 93 (2019) e00520-19. https://doi.org/10.1128/JVI.00520-19.

[19] B. Monel, A.A. Compton, T. Bruel, S. Amraoui, J. Burlaud-Gaillard, N. Roy, F. Guivel-Benhassine, F. Porrot, P. Génin, L. Meertens, L. Sinigaglia, N. Jouvenet, R. Weil, N. Casartelli, C. Demangel, E. Simon-Lorière, A. Moris, P. Roingeard, A. Amara, O. Schwartz, Zika virus induces massive cytoplasmic vacuolization and paraptosis-like death in infected cells, EMBO J. 36 (2017) 1653–1668. https://doi.org/10.15252/embj.201695597.

[20] I. Umareddy, O. Pluquet, Q.Y. Wang, S.G. Vasudevan, E. Chevet, F. Gu, , Virol. J. 4 (2007) 91. https://doi.org/10.1186/1743-422X-4-91.

[21] H.-L. Su, C.-L. Liao, Y.-L. Lin, Japanese encephalitis virus infection initiates endoplasmic reticulum stress and an unfolded protein response, J. Virol. 76 (2002) 4162–4171. https://doi.org/10.1128/jvi.76.9.4162-4171.2002.

[22] Y.-R. Lee, S.-H. Kuo, C.-Y. Lin, P.-J. Fu, Y.-S. Lin, T.-M. Yeh, H.-S. Liu, Dengue virus-induced ER stress is required for autophagy activation, viral replication, and pathogenesis both in vitro and in vivo, Sci. Rep. 8 (2018) 1–14. https://doi.org/10.1038/s41598-017-18909-3.

[23] J. Peña, E. Harris, Dengue virus modulates the unfolded protein response in a time-dependent manner, J. Biol. Chem. 286 (2011) 14226–14236. https://doi.org/10.1074/jbc.M111.222703.

[24] G.R. Medigeshi, A.M. Lancaster, A.J. Hirsch, T. Briese, W.I. Lipkin, V. Defilippis, K. Früh, P.W. Mason, J. Nikolich-Zugich, J.A. Nelson, West Nile virus infection activates the unfolded protein response, leading to CHOP induction and apoptosis, J. Virol. 81 (2007) 10849–10860. https://doi.org/10.1128/JVI.01151-07.

[25] E. Frumence, M. Roche, P. Krejbich-Trotot, C. El-Kalamouni, B. Nativel, P. Rondeau, D. Missé, G. Gadea, W. Viranaicken, P. Desprès, The South Pacific epidemic strain of Zika virus replicates efficiently in human epithelial A549 cells leading to IFN-β production and apoptosis induction, Virology. 493 (2016) 217–226. https://doi.org/10.1016/j.virol.2016.03.006.

[26] C. El Kalamouni, E. Frumence, S. Bos, J. Turpin, B. Nativel, W. Harrabi, D.A. Wilkinson, O. Meilhac, G. Gadea, P. Desprès, P. Krejbich-Trotot, W. Viranaïcken, Subversion of the Heme Oxygenase-1 Antiviral Activity by Zika Virus, Viruses. 11 (2018). https://doi.org/10.3390/v11010002.

[27] W. Viranaicken, B. Nativel, P. Krejbich-Trotot, W. Harrabi, S. Bos, C. El Kalamouni, M. Roche, G. Gadea, P. Desprès, ClearColi BL21(DE3)-based expression of Zika virus antigens illustrates a rapid method of antibody production against emerging pathogens, Biochimie. 142 (2017) 179–182. https://doi.org/10.1016/j.biochi.2017.09.011.

[28] J. ichi Nozaki, H. Kubota, H. Yoshida, M. Naitoh, J. Goji, T. Yoshinaga, K. Mori, A. Koizumi, K. Nagata, The endoplasmic reticulum stress response is stimulated through the continuous activation of transcription factors ATF6 and XBP1 in Ins2+/Akita pancreatic β cells, Genes Cells. 9 (2004) 261–270. https://doi.org/10.1111/j.1356-9597.2004.00721.x.

[29] W. Viranaicken, L. Gasmi, A. Chaumet, C. Durieux, V. Georget, P. Denoulet, J.-C. Larcher, L-Ilf3 and L-NF90 Traffic to the Nucleolus Granular Component: Alternatively-Spliced Exon 3 Encodes a Nucleolar Localization Motif, PLoS ONE. 6 (2011). https://doi.org/10.1371/journal.pone.0022296.

[30] J.L. Muñoz-Jordan, G.G. Sánchez-Burgos, M. Laurent-Rolle, A. García-Sastre, Inhibition of interferon signaling by dengue virus, Proc. Natl. Acad. Sci. U. S. A. 100 (2003) 14333–14338. https://doi.org/10.1073/pnas.2335168100.

[31] S. Bos, W. Viranaicken, J. Turpin, C. El-Kalamouni, M. Roche, P. Krejbich-Trotot, P. Desprès, G. Gadea, The structural proteins of epidemic and historical strains of Zika virus differ in their ability to initiate viral infection in human host cells, Virology. 516 (2018) 265–273. https://doi.org/10.1016/j.virol.2017.12.003.

[32] J. Turpin, E. Frumence, P. Desprès, W. Viranaicken, P. Krejbich-Trotot, The ZIKA Virus Delays Cell Death Through the Anti-Apoptotic Bcl-2 Family Proteins, Cells. 8 (2019) 1338. https://doi.org/10.3390/cells8111338.

[33] A. Saito, K. Imaizumi, Unfolded Protein Response-Dependent Communication and Contact among Endoplasmic Reticulum, Mitochondria, and Plasma Membrane, Int. J. Mol. Sci. 19 (2018) 3215. https://doi.org/10.3390/ijms19103215.

[34] H. Urra, E. Dufey, F. Lisbona, D. Rojas-Rivera, C. Hetz, When ER stress reaches a dead end, Biochim. Biophys. Acta BBA - Mol. Cell Res. 1833 (2013) 3507–3517. https://doi.org/10.1016/j.bbamcr.2013.07.024.

[35] C.M. Oslowski, F. Urano, Measuring ER stress and the unfolded protein response using mammalian tissue culture system, Methods Enzymol. 490 (2011) 71–92. https://doi.org/10.1016/B978-0-12-385114-7.00004-0.

[36] T. Okamoto, T. Suzuki, S. Kusakabe, M. Tokunaga, J. Hirano, Y. Miyata, Y. Matsuura, Regulation of Apoptosis during Flavivirus Infection, Viruses. 9 (2017). https://doi.org/10.3390/v9090243.

## Figure Legends

**Figure 1. ER morphological features during ZIKV infection.** A549 cells were infected with ZIKV at MOI of 1 for 48h. Cells were immunostained for calnexin and E-ZIKV. Scale bar: 5 µm. Right panel series show magnified details of a selected cell from the x200 microscopic field (white square). All experiments were representative of three independent experiments.

**Figure 2. UPR branch activation during ZIKV infection. (A)** A549 cells were infected with ZIKV at MOI of 1 for 24h. RT-PCR were performed to monitor transcriptional regulation of downstream gene targets of the UPR branch, chop (PERK branch), xbp1 splicing (IRE1 branch) and grp78 (ATF6 branch). u-xbp1 correspond to unspliced xbp1 and s-xbp1 to spliced Xbp1. **(B)** A549 cells infected with ZIKV at indicated MOI for 48h were lysed in buffer A, total protein extracts, under reducing conditions were immuno-blotted for E-ZIKV with EDIII antibody, GRP78 and β-tubulin as a loading control. **(C)** A549 cells ($1x10^6$ cells) were transfected with the indicated reporter constructs. After 12h, transfected cells were plated at a density of $3x10^4$ cells per well and infected with ZIKV at MOI of 5. Luciferase activities were measured 24h post infection. Degrees of significance are indicated in the figure captions as follow: * $p < 0.05$; ** $p < 0.01$; *** $p < 0.001$, **** $p < 0.0001$, ns = not significant. For all experiments Thapsigargin-ER stress induced (TG) were used as positive control at 1 µM for 6h. RT-PCR and western blot experiments were representative of three independent experiments.

**Figure 3. Crosstalk between UPR and ZIKV during infection. (A)** A549 cells were infected with ZIKV at MOI of 5 for 18h. 2h post-infection tunicamycin (TM) was added at the indicated concentration. After RNA extraction, qRT-PCR were realized to quantify viral genomic RNA copies. **(B)** Viral progeny production in cell culture supernatants of cells infected and treated with TM were determined by PFU assay (left axis). **(C)** Total protein extract under reducing conditions were immuno-blotted for E-ZIKV with EDIII antibody, GRP78 and β-tubulin as a loading control. Cell mortality was evaluated through LDH release and absorbance measurement (right axis). **(D)** A549 cells were infected or not with ZIKV for 16h at MOI of 5, followed by 4h treatment with TG at 1µM. Western blot were performed on total extract as in (A). All results were representative of three independent experiments.

Figure 1

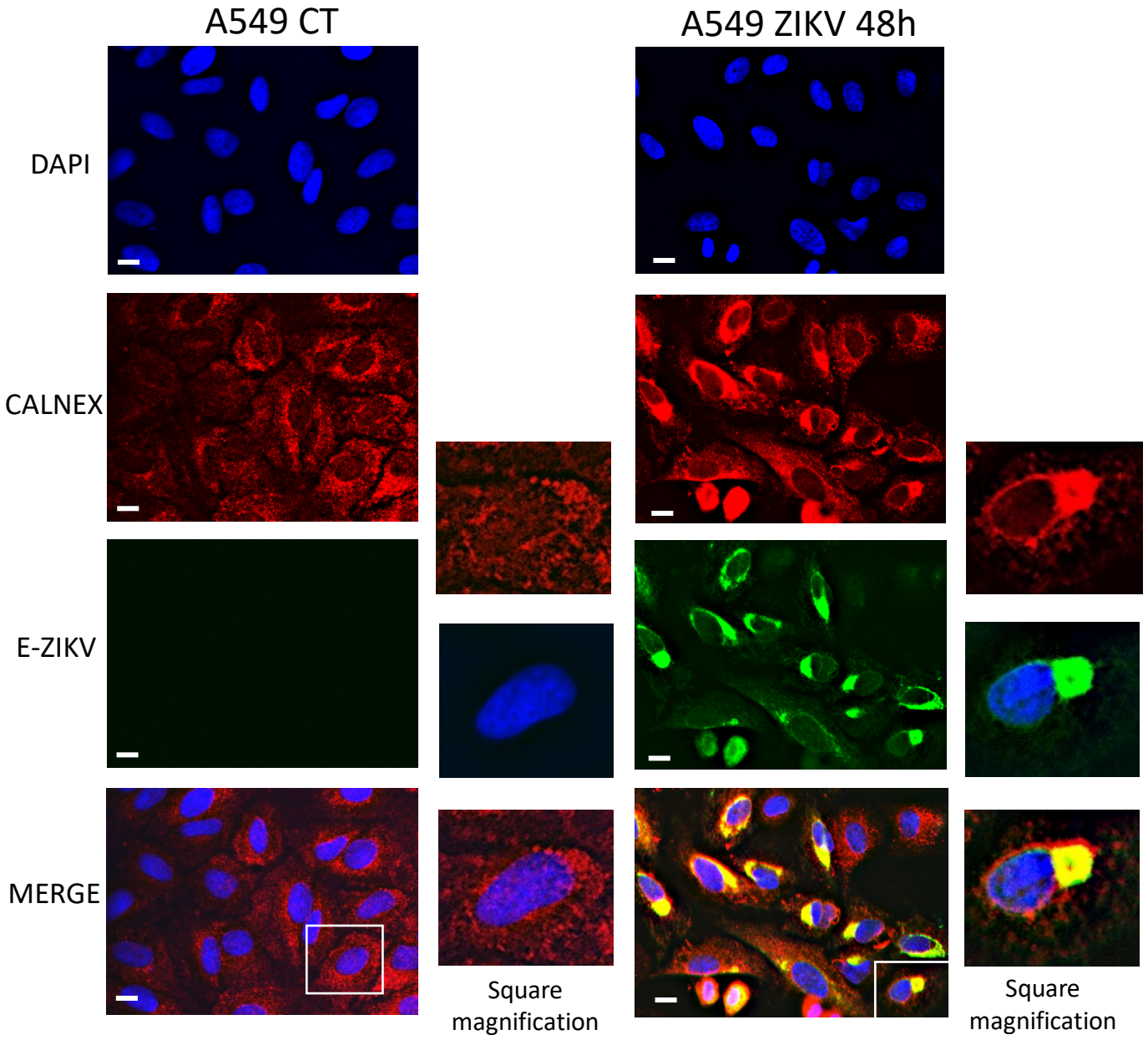
A549 CT
A549 ZIKV 48h
DAPI
CALNEX
E-ZIKV
MERGE
Square magnification
Square magnification

Figure 2

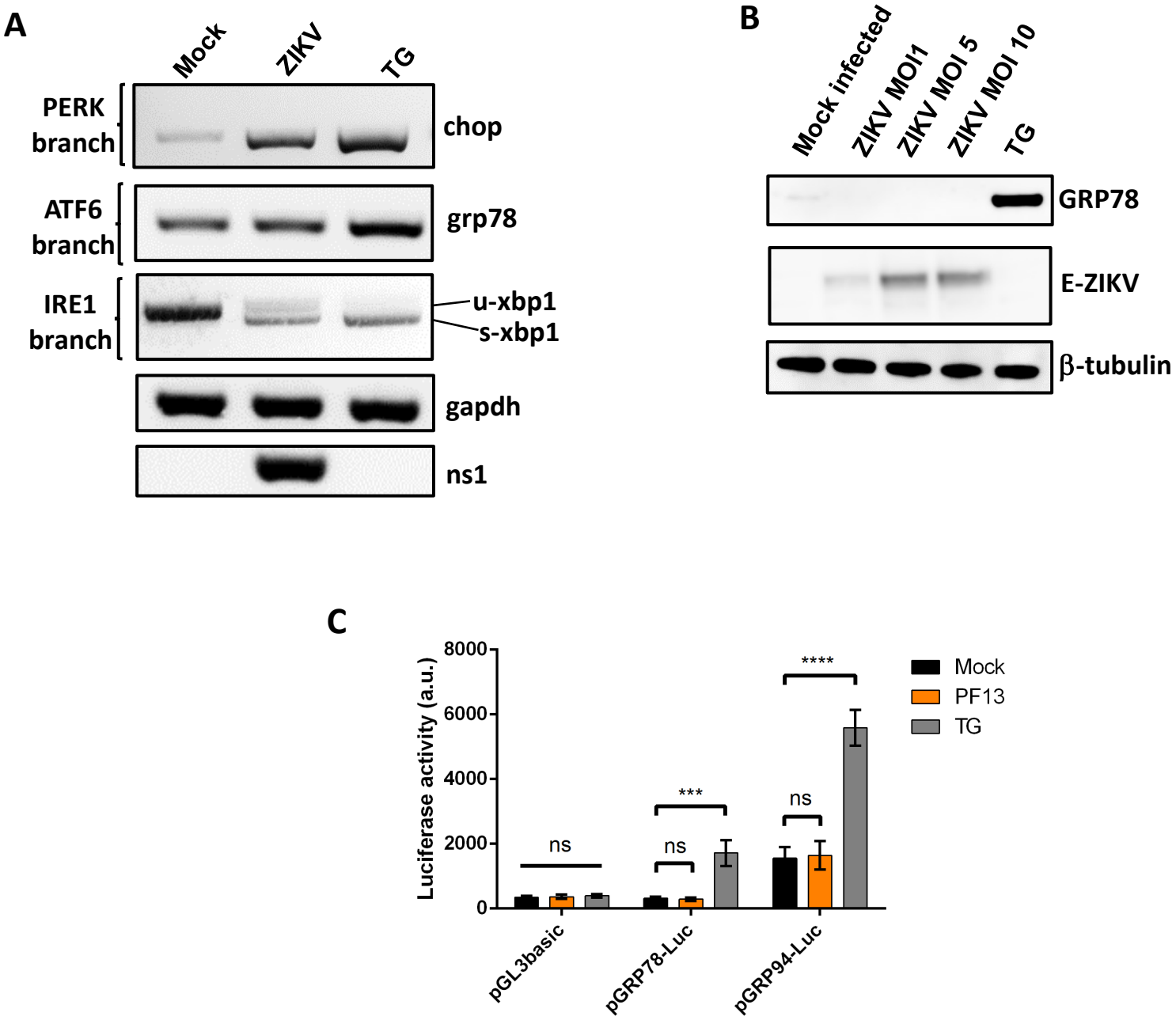
A
Mock
ZIKV
TG
PERK branch
chop
ATF6 branch
grp78
IRE1 branch
u-xbp1
s-xbp1
gapdh
ns1
B
Mock infected
ZIKV MOI1
ZIKV MOI 5
ZIKV MOI 10
TG
GRP78
E-ZIKV
β-tubulin
C
Luciferase activity (a.u.)
8000
6000
4000
2000
0
ns
***
ns
****
ns
Mock
PF13
TG
pGL3basic
pGRP78-Luc
pGRP94-Luc

Figure 3

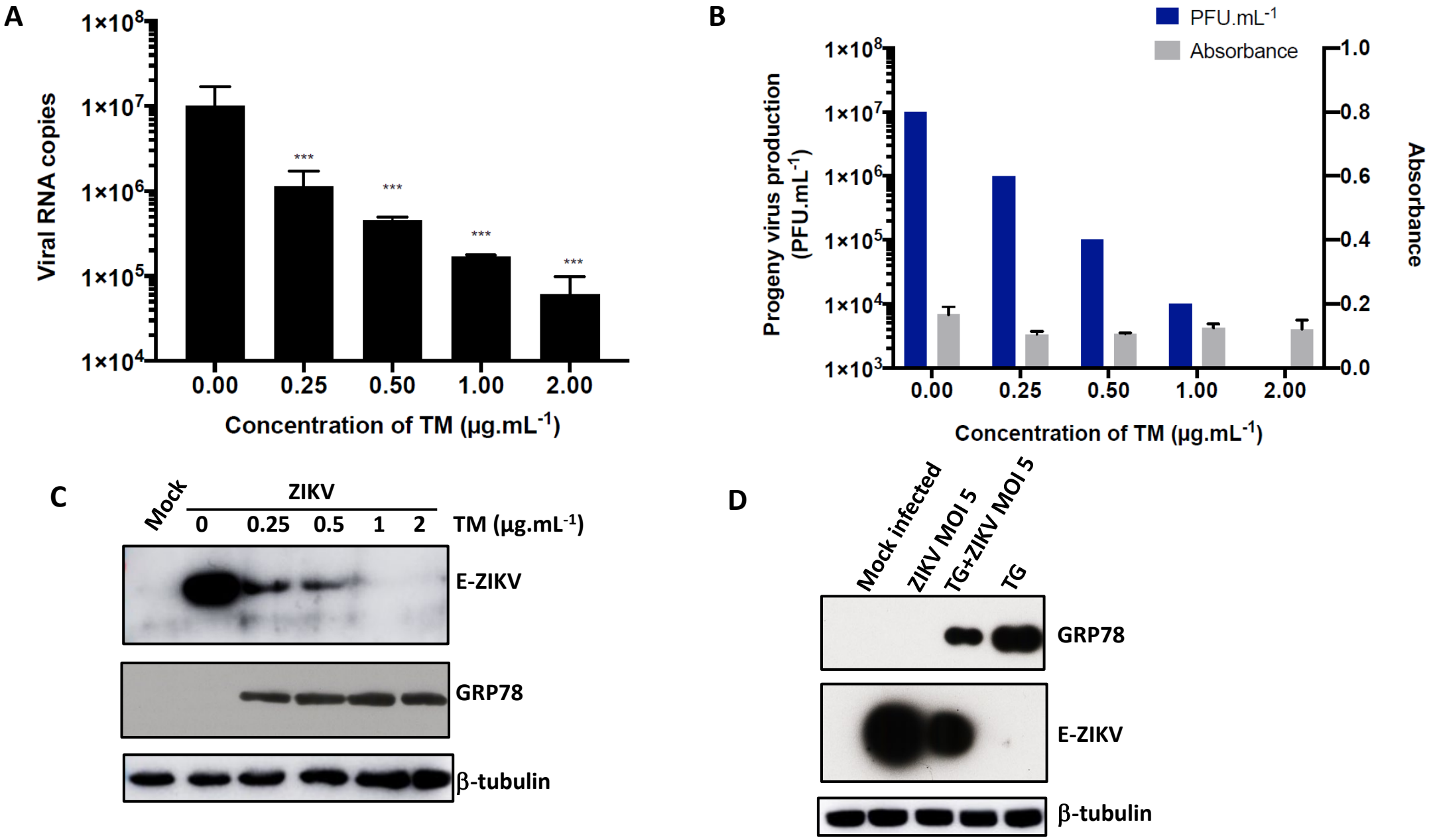
A
Viral RNA copies
1×10^8
1×10^7
1×10^6
1×10^5
1×10^4
***
***
***
***
0.00
0.25
0.50
1.00
2.00
Concentration of TM (μg.mL^-1)
B
PFU.mL^-1
Absorbance
Progeny virus production (PFU.mL^-1)
1×10^8
1×10^7
1×10^6
1×10^5
1×10^4
1×10^3
1.0
0.8
0.6
0.4
0.2
0.0
Absorbance
0.00
0.25
0.50
1.00
2.00
Concentration of TM (μg.mL^-1)
C
Mock
ZIKV
0
0.25
0.5
1
2
TM (μg.mL^-1)
E-ZIKV
GRP78
β-tubulin
D
Mock infected
ZIKV MOI 5
TG+ZIKV MOI 5
TG
GRP78
E-ZIKV
β-tubulin

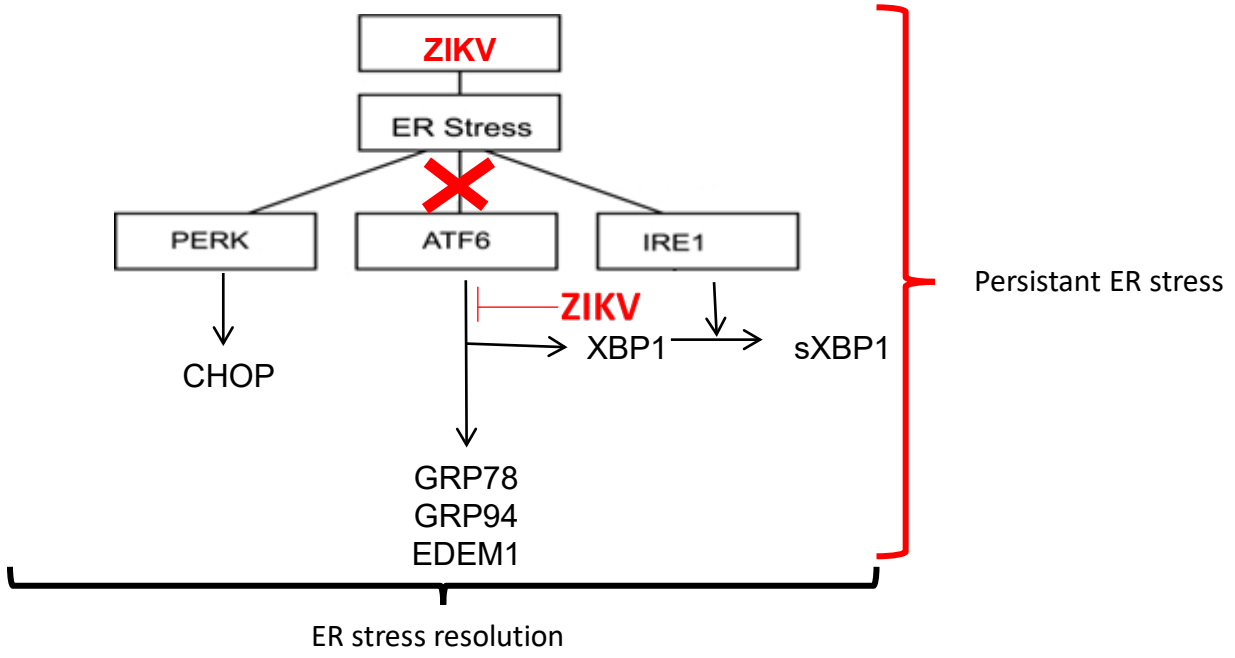


Graphical abstract